



# A generalized Fourier domain: Signal processing framework and applications



Jorge Martinez\*, Richard Heusdens, Richard C. Hendriks

Signal and Information Processing (SIP) Lab, Delft University of Technology, Mekelweg 4, 2628CD Delft, Netherlands

## ARTICLE INFO

### Article history:

Received 9 August 2011

Received in revised form

18 October 2012

Accepted 24 October 2012

Available online 2 November 2012

### Keywords:

Generalized Fourier domain

Generalized discrete Fourier transform

Weighted circular convolution

## ABSTRACT

In this paper, a signal processing framework in a generalized Fourier domain (GFD) is introduced. In this newly proposed domain, a parametric form of control on the periodic repetitions that occur due to sampling in the reciprocal domain is possible, without the need to increase the sampling rate. This characteristic and the connections of the generalized Fourier transform to analyticity and to the  $z$ -transform are investigated. Core properties of the generalized discrete Fourier transform (GDFT) such as a weighted circular correlation property and Parseval's relation are derived. We show the benefits of using the novel framework in a spatial-audio application, specifically the simulation of room impulse responses for auralization purposes in e.g. virtual reality systems.

© 2012 Elsevier B.V. All rights reserved.

## 1. Introduction

In this paper we introduce a framework for signal processing in a generalized Fourier domain (GFD). In this domain a special form of control on the periodic repetitions that occur due to sampling in the reciprocal domain is possible, without the need to increase the sampling rate. First in Section 2 we review the definition of the generalized discrete Fourier transform (GDFT) and its associated generalized Poisson summation formula (GPSF), both previously introduced in [1]. Analogous to the periodic extension of a finite-length signal that occurs in standard Fourier theory [2,3], here we introduce the concept of “weighted periodic signal extension” that naturally occurs when working in the GFD. Next we study the connections of the presented theory to spectral sampling, analyticity and the  $z$ -transform. This analysis also serves as a discussion of the generalized Fourier transform and its relationship to the standard Fourier transform. In Section 3 important properties of the GDFT

are derived such as the *weighted* circular correlation property and Parseval's energy relation for the GFD that, together with the previously introduced *weighted* circular convolution theorem for the GDFT, are fundamental to build a general-purpose GFD-based signal processing framework. To finalize our discussion in Section 4 we show how the novel framework can be used in spatial-audio applications such as the simulation of multichannel room impulse responses for auralization purposes in e.g. virtual reality and telegaming systems.

## 2. A generalized Fourier domain

Let us define the generalized discrete Fourier transform for finite-length signals  $x(n)$ ,  $n = \{0, \dots, N-1\}$ , with parameter  $\alpha \in \mathbb{C} \setminus \{0\}$  as,

$$\mathcal{F}_\alpha\{x(n)\} \triangleq X_\alpha(k) = \sum_{n=0}^{N-1} x(n)e^{\beta n} e^{-j(2\pi/N)kn}, \quad (1)$$

for  $k = \{0, \dots, N-1\}$ , where  $\beta = \log(\alpha)/N$ . The inverse GDFT is given by [1],

$$\mathcal{F}_\alpha^{-1}\{X_\alpha(k)\} \triangleq x(n) = \frac{e^{-\beta n}}{N} \sum_{k=0}^{N-1} X_\alpha(k) e^{j(2\pi/N)kn}. \quad (2)$$

\* Corresponding author. Tel.: +31 15 27 82 188;

fax: +31 15 27 81 843.

E-mail address: J.A.MartinezCastaneda@TuDelft.nl (J. Martinez).

URL: <http://siplab.tudelft.nl> (J. Martinez).

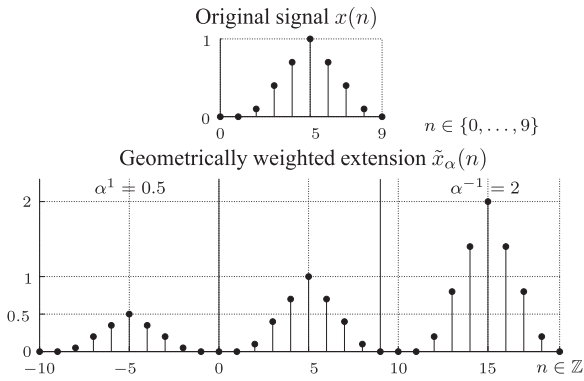


**Fig. 1.** Geometrically weighted extension of a finite length signal when evaluated outside its original domain, for  $\alpha = 0.5$  and  $N = 10$ .

The GDFT (1) is equivalent to the ordinary discrete Fourier transform of the modulated signal  $x(n)e^{j\beta n}$ . The finite-length signal  $e^{j\beta n}$  for  $n = \{0, \dots, N-1\}$ , is of finite energy for all  $\alpha \in \mathbb{C} \setminus \{0\}$ , therefore for  $x(n)$  a signal of finite energy, the GDFT can be properly defined [2,1]. Note that when  $\alpha = 1$ , the transform pair correspond to the standard DFT pair.

Let us denote the periodic extension of  $X_x(k)$  by  $\tilde{X}_x(k)$  for  $k \in \mathbb{Z}$ . Clearly we have that  $\tilde{X}_x(k) = X_x(k)_N$ , where  $X_x(k)_N \triangleq X_x(k \bmod N)$ , i.e. the circular shift of the sequence is represented as the index modulo  $N$ . On the other hand (1) and (2) imply a geometrically weighted periodic extension of the signal  $x(n)$  when evaluated outside  $\{0, \dots, N-1\}$ . This is stated by the generalized Poisson summation formula (GPSF) associated with the transform [1],

$$\tilde{x}_x(n) \triangleq \sum_{p \in \mathbb{Z}} \alpha^p x(n) N = \frac{e^{-\beta n}}{N} \sum_{k=0}^{N-1} X_x(k) e^{i(2\pi/N)kn}, \quad (3)$$

where  $n \in \mathbb{Z}$ ,  $p = -\lfloor n/N \rfloor$  and  $((n))_N = n + pN$ . We can regard  $\tilde{x}_x(n)$  as a superposition of infinitely many translated and geometrically weighted “replicas” of  $x(n)$ . The replicas outside the support of  $x(n)$  are weighted by  $\alpha^p$  and  $\tilde{x}_x(n) = x(n)$  for  $n = \{0, \dots, N-1\}$ . This is illustrated in Fig. 1, where a finite signal and (a part of) its geometrically weighted extension are depicted for  $\alpha = 0.5$  and  $N = 10$ . Therefore to work in the generalized Fourier domain implies a manipulation of the signals involved via their geometrically weighted extensions. This is an important fact as we will see through the rest of the paper.

Signals of the form  $\tilde{x}_x(n)$  although infinitely long and not being of finite energy can be decomposed into its generalized Fourier transform components by means of (1), evaluating the transform over a signal interval (“period”) of length  $N$ . This fact follows directly from the generalized Poisson summation formula (3) which shows, that the inverse transform  $(\exp(-\beta n)/N) \sum_{k=0}^{N-1} X_x(k) \exp(j(2\pi/N)kn)$  is of the form  $\tilde{x}_x(n)$  when evaluated over  $n = \mathbb{Z}$ .

2.1. Connection to sampling, analyticity and the z-transform

The summation formula (3) has an important relationship to spectral sampling. The connection of the (discrete-time) generalized Fourier transform to analyticity and to the z-transform follows as part of the analysis. These

relationships are used in a practical application of the theory in Section 4.

Let us begin with the connection to analyticity. Define the standard spectrum of a discrete-time signal by  $S(\omega)$ , where  $\omega \in \mathbb{R}$  represents angular frequency and let  $S(\omega) \in L^2[-\pi, \pi]$ . Since the original signal  $s(n)$ ,  $n \in \mathbb{Z}$ , is defined for discrete-time it is clear that  $S(\omega)$  is a periodic function of  $\omega$  with period equal to  $2\pi$ . The signal  $s(n)$  could represent the samples of a continuous-time signal, but without the sampling interval that information is lost and no particular analog representation is to be inferred. Let us assume for a moment that  $S(\omega)$  can be analytically continued into the complex angular-frequency plane. This is  $S(\omega) \rightarrow S(\omega_z)$ , where  $\omega_z \in \mathbb{C}$  is the complex-valued angular frequency. Let  $\omega_r$  and  $\omega_i$  denote the real and imaginary parts respectively of  $\omega_z$ . Then from the definition of the discrete-time Fourier transform we have,

$$\begin{aligned} S(\omega_z) &= \sum_{n=-\infty}^{\infty} s(n)e^{-j\omega_z n}, \\ S(\omega_r + j\omega_i) &= \sum_{n=-\infty}^{\infty} s(n)e^{-j(\omega_r + j\omega_i)n}, \\ S(\omega_r + j\omega_i) &= \sum_{n=-\infty}^{\infty} s(n)e^{\omega_i n} e^{-j\omega_r n}. \end{aligned} \quad (4)$$

From here we see that if  $s(n)$  is a causal sequence and the analytic continuation of  $S(\omega)$  is done on the lower half of the complex plane then  $\omega_i < 0$ ,

$$S(\omega_r + j\omega_i) = \sum_{n=0}^{\infty} s(n)e^{\omega_i n} e^{-j\omega_r n},$$

and the extra factor  $e^{\omega_i n}$  can only improve the convergence rate of the series. Now,

$$\begin{aligned} \lim_{\omega_i \rightarrow -0} S(\omega_r + j\omega_i) &= \lim_{\omega_i \rightarrow -0} \sum_{n=0}^{\infty} s(n)e^{-j\omega_r n + \omega_i n}, \\ &= \sum_{n=0}^{\infty} \lim_{\omega_i \rightarrow -0} s(n)e^{-j\omega_r n + \omega_i n}, \\ &= S(\omega). \end{aligned}$$

On the other hand we have that

$$\begin{aligned} &\int_{-\pi}^{\pi} |S(\omega_r + j\omega_i)|^2 d\omega_r \\ &= \int_{-\pi}^{\pi} S(\omega_r + j\omega_i) S^*(\omega_r + j\omega_i) d\omega_r, \\ &= \int_{-\pi}^{\pi} \left( \sum_{n=0}^{\infty} s(n)e^{-j\omega_r n + \omega_i n} \sum_{m=0}^{\infty} s^*(m)e^{j\omega_r m + \omega_i m} \right) d\omega_r, \\ &= \sum_{n=0}^{\infty} \left( s(n)e^{\omega_i n} \sum_{m=0}^{\infty} s^*(m)e^{\omega_i m} \int_{-\pi}^{\pi} e^{j\omega_r(m-n)} d\omega_r \right), \\ &= 2\pi \sum_{n=0}^{\infty} s(n)e^{\omega_i n} s^*(n)e^{\omega_i n}, \\ &= 2\pi \sum_{n=0}^{\infty} |s(n)|^2 e^{2\omega_i n} < 2\pi \sum_{n=0}^{\infty} |s(n)|^2, \end{aligned}$$

where  $*$  denotes complex conjugation. Recalling Parseval’s relation and noting that  $S(\omega) \in L^2[-\pi, \pi]$  implies  $s(n) \in l^2(\mathbb{Z})$  [3,2], then for a positive constant  $C$ ,

$$\int_{-\pi}^{\pi} |S(\omega_r + j\omega_i)|^2 d\omega_r < C.$$

The function  $S(\omega_r + j\omega_i)$  is the analytic continuation from the real line into the lower half of the complex plane of the spectrum of the causal signal  $s(n)$ . By the same arguments if  $s(n) = 0$  for  $n > 0$  (i.e. is an anticausal signal), then its spectrum admits analytic continuation into the upper half of the complex angular-frequency plane.

Define now a discrete-time generalized Fourier transform as,

$$S_x(\omega) = \sum_{n=-\infty}^{\infty} s(n)e^{\beta n} e^{-j\omega n}, \quad (5)$$

with inverse transformation,

$$s(n) = \frac{e^{-\beta n}}{2\pi} = \int_{-\pi}^{\pi} S_x(\omega)e^{j\omega n} d\omega, \quad (6)$$

where, as in (1),  $\beta = \log(\alpha)/N$  and  $\alpha \in \mathbb{C}/\{0\}$ . By our previous discussion we can write

$$S_x(\omega) = S(\omega + j\beta) = S(\omega - \beta_i + j\beta_r),$$

where  $\beta_r$  and  $\beta_i$  are the real and imaginary parts respectively of parameter  $\beta$ . Clearly if  $\beta_r < 0$  (or equivalently  $|\alpha| < 1$ ) the transform is well defined for causal signals. In the same way if  $\beta_r > 0$  (i.e.  $|\alpha| > 1$ ) the transform is well defined for anticausal signals. In both cases the generalized spectrum can be obtained via analytic continuation (into the proper half of the complex plane) of the standard Fourier spectrum. Also note that  $\beta_i$  implies a frequency shift. If the principal value of  $\log(\alpha)$  is to be taken this shift is limited from  $-\pi/N$  to  $\pi/N$ .

Recall now the definition of the z-transform,

$$S(z) = \sum_{n=-\infty}^{\infty} s(n)z^{-n}.$$

Since parameter  $\alpha$  is constant, we find the transform (5) to be a particular case of the z-transform, with  $z = e^{-\beta_r - j(\beta_i - \omega)}$ . This implies  $|z| = |\alpha|^{-1/N}$ , with the real positive Nth-root being the only root satisfying the equation. The discrete-time GFT can be viewed as the z-transform of the signal evaluated on a circle of radius  $|\alpha|^{-1/N}$ . When  $|\alpha| = 1$  the evaluation is done on the unit circle and the GFT is equivalent to the standard Fourier transform shifted in frequency, this is,  $S_x(\omega) = S(\omega - \theta/N)$ , with  $\alpha = e^{j\theta}$ . We can now extend the definition of the GFT to signals other than single-sided (causal or anticausal). If the z-transform of the signal has a region of convergence that includes the circle of radius  $|\alpha|^{-1/N}$ , then the GFT exists. Note that finite-length signals have as region of convergence the whole z-plane with exception of the points  $z = 0$  and/or  $z = \infty$ . Since  $\alpha \in \mathbb{C}/\{0\}$  the GFD always exists for finite-length signals of finite energy.

The relationship of (3) to spectral sampling is now explored. Since  $S_x(\omega)$  is a periodic function of  $\omega$  the integral in (6) can be taken over any interval of length  $2\pi$ . To make the derivation simpler let

$$s(n) = \frac{e^{-\beta n}}{2\pi} = \int_0^{2\pi} S_x(\omega)e^{j\omega n} d\omega.$$

The integral can be approximated using a rectangular quadrature rule, dividing the integration interval uniformly into  $N$  subintervals and using the samples of the integrand at the

subinterval points. Let  $2\pi/N$  be the sampling interval, then

$$\int_0^{2\pi} S_x(\omega)e^{j\omega n} d\omega \approx \frac{2\pi}{N} \sum_{k=0}^{N-1} S_x\left(\frac{2\pi}{N}k\right) e^{j(2\pi/N)nk}.$$

An approximation of  $s(n)$ , call it  $\tilde{s}_x(n)$ , is thus obtained as

$$\tilde{s}_x(n) = \frac{e^{-\beta n}}{N} \sum_{k=0}^{N-1} S_x\left(\frac{2\pi}{N}k\right) e^{j(2\pi/N)nk}.$$

Substituting (5) into this last expression reveals the connection of  $\tilde{s}_x(n)$  to the original signal  $s(n)$ ,

$$\begin{aligned} \tilde{s}_x(n) &= \frac{e^{-\beta n}}{N} \sum_{k=0}^{N-1} \left( \sum_{m=-\infty}^{\infty} s(m)e^{\beta m} e^{-j(2\pi/N)km} \right) e^{j(2\pi/N)kn} \\ &= \frac{e^{-\beta n}}{N} \sum_{m=-\infty}^{\infty} s(m)e^{\beta m} \left( \sum_{k=0}^{N-1} e^{j(2\pi/N)k(n-m)} \right). \end{aligned}$$

For  $p \in \mathbb{Z}$ ,  $p = -\lfloor n/N \rfloor$  we have [3],

$$\sum_{k=0}^{N-1} e^{j(2\pi/N)k(n-m)} = \begin{cases} N, & m = n + pN, \\ 0, & \text{otherwise.} \end{cases}$$

Then

$$\begin{aligned} \tilde{s}_x(n) &= e^{-\beta n} \sum_{p=-\infty}^{\infty} s(n+pN)e^{\beta(n+pN)} \\ &= \sum_{p=-\infty}^{\infty} s(n+pN)e^{\beta pN} = \sum_{p=-\infty}^{\infty} \alpha^p s(n+pN). \end{aligned}$$

So that

$$\tilde{s}_x(n) = \sum_{p=-\infty}^{\infty} \alpha^p s(n+pN) = \frac{e^{-\beta n}}{N} \sum_{k=0}^{N-1} S_x\left(\frac{2\pi}{N}k\right) e^{j(2\pi/N)nk}.$$

We have arrived to the generalized Poisson summation formula (3), which states that uniform spectral sampling of the generalized Fourier spectrum  $S_x(\omega)$  implies a geometrically weighted periodic summation of the original discrete-time signal  $s(n)$ . This property is used in a spatial-audio application in Section 4, but first we analyze some properties of the GDFT.

### 3. Properties of the GDFT

In this section we present some important properties of the GDFT, these are a fundamental part in any GFD-based signal processing framework. In the following let  $x(n)$  and  $y(n)$  for  $n = \{0, \dots, N-1\}$  be two finite-duration and in general complex signals of length  $N$ , and  $X_x(k)$  and  $Y_x(k)$  for  $k = \{0, \dots, N-1\}$  their respective GDFTs.

**Property 1.** *Weighted circular convolution. Point-wise multiplication of  $X_x(k)$  and  $Y_x(k)$  in the GFD corresponds to the weighted circular convolution of  $x(n)$  and  $y(n)$  in the time domain, i.e.*

$$\begin{aligned} \mathcal{F}_\alpha^{-1}\{X_x(k)Y_x(k)\} &= \frac{e^{-\beta n}}{N} \sum_{k=0}^{N-1} X_x(k)Y_x(k)e^{j(2\pi/N)nk} \\ &= \sum_{m=0}^{N-1} x(m)\tilde{y}_x(n-m), \end{aligned}$$

$$\begin{aligned} \mathcal{F}_\alpha^{-1}\{X_\alpha(k)Y_\alpha(k)\} &= \sum_{m=0}^{N-1} x(m)\alpha^p y(n-m+pN) \\ &= \sum_{m=0}^{N-1} x(m)\alpha^p y((n-m))_N, \end{aligned} \quad (7)$$

or

$$(x*\tilde{y}_\alpha)(n) \xleftrightarrow{\mathcal{F}_\alpha} X_\alpha(k)Y_\alpha(k),$$

where  $*$  is the linear convolution operator. The operation can thus be seen as the linear convolution of one of the signals e.g.  $x(n)$ , with the respective signal extension of the other,  $\tilde{y}_\alpha(n)$ . Note that for  $n = \{0, \dots, N-1\}$  we have that  $(n-m) \in \{-N+1, \dots, N-1\}$ , and thus  $p \in \{0, 1\}$ , so that (7) can be rewritten as

$$\sum_{m=0}^n x(m)y(n-m) + \alpha \sum_{m=n+1}^{N-1} x(m)y(N+n-m), \quad (8)$$

where the left hand summation represents the contribution of  $N$  linear convolution terms, and the right hand summation the contribution of  $N$  circular convolution terms (which are in fact the last terms of the linear convolution). The factor  $\alpha$  effectively weights the amount of circular convolution that is obtained. The proof is given in [1]. Property 1 can be exploited to compute linear convolutions in the GFD without the need of zero-padding, using GDFTs with e.g. parameter  $\alpha = \pm j$  or  $\alpha \leq 1 \in \mathbb{R}$ , [1].

Next we present the shifting properties for the GDFT, the first accounts for a shift in the time-domain the second for a shift in the GFD.

**Property 2. Time-domain shift.**

For  $n_0 \in \mathbb{Z}$ ,

$$\tilde{x}_\alpha(n-n_0) \xleftrightarrow{\mathcal{F}_\alpha} e^{j\beta n_0} e^{-j(2\pi/N)kn_0} X_\alpha(k).$$

The GDFT with parameter  $\alpha$  of the shifted signal  $\tilde{x}_\alpha(n-n_0)$  is equal to the modulated generalized spectrum of the original signal  $x(n)$ . The proof is given in Appendix A.

**Property 3. GFD shift.** For  $k_0 \in \mathbb{Z}$ ,

$$x(n)e^{j(2\pi/N)k_0 n} \xleftrightarrow{\mathcal{F}_\alpha} \tilde{X}_\alpha(k-k_0) = X_\alpha((k-k_0))_N.$$

To circularly shift the generalized spectrum  $X_\alpha(k)$  of a signal is equivalent in the time-domain to modulate the signal with the function  $e^{j(2\pi/N)k_0 n}$ . The proof is given in Appendix B.

**Property 4. Time reversal.**

$$\tilde{x}_\alpha(-n) \xleftrightarrow{\mathcal{F}_\alpha^{-1}} \tilde{X}_\alpha(-k).$$

The GDFT with parameter  $\alpha^{-1}$  of the time-reversed extension of  $x$  with parameter  $\alpha$ ,  $\tilde{x}_\alpha(-n)$ , is thus equivalent to reversing (modulo  $N$ ) the GDFT of  $x(n)$  with parameter  $\alpha$ . This result is a direct consequence of the reciprocal-symmetric structure of the signal extension  $\tilde{x}_\alpha(n)$  with

respect to  $\alpha$ . Notice that if the extension is time reversed the geometrically weighted “replicas” outside the support of  $x(-n)$  no longer correspond to a weight  $\alpha^p$  but to  $\alpha^{-p}$ . Therefore to obtain Property 4 a GDFT with parameter  $\alpha^{-1}$  has to be applied to the time reversed extension,  $\tilde{x}_\alpha(-n)$ . The proof is given in Appendix C.

**Property 5. Time domain complex-conjugate.**

$$x^*(n) \xleftrightarrow{\mathcal{F}_\alpha} \tilde{X}_\alpha^*(-k).$$

To take the inverse GDFT with parameter  $\alpha^*$  of  $\tilde{X}_\alpha^*(-k)$  is equivalent to take the complex conjugate of the time domain signal  $x^*(n)$ . The proof is given in Appendix D.

Consider that the real part of a complex signal is given by  $\Re\{x(n)\} = (1/2)(x(n)+x^*(n))$ , and its imaginary part is given by  $\Im\{x(n)\} = (1/2j)(x(n)-x^*(n))$ . The last property (making  $\alpha \rightarrow \alpha^*$ ) can then be used to derive the following results,

$$\Re\{x(n)\} \xleftrightarrow{\mathcal{F}_\alpha} \frac{1}{2}(X_\alpha + \tilde{X}_{\alpha^*}^*(-k)).$$

The real part of a complex signal  $x(n)$  can be obtained by taking the inverse GDFT with parameter  $\alpha$  of a linear combination of the GDFT of  $x(n)$  with parameter  $\alpha$ , and the GDFT of  $x(n)$  with parameter  $\alpha^*$  conjugated and reversed (modulo  $N$ ). Correspondingly we also have that,

$$\Im\{x(n)\} \xleftrightarrow{\mathcal{F}_\alpha} \frac{1}{2j}(X_\alpha - \tilde{X}_{\alpha^*}^*(-k)).$$

**Property 6. GFD complex-conjugate.**

$$\tilde{x}_\alpha^*(-n) \xleftrightarrow{\mathcal{F}_\alpha} X_\alpha^*(k),$$

where  $\alpha^{-*} = (\alpha^*)^{-1}$ . To take the complex conjugate of the spectrum,  $X_\alpha^*(k)$  is equivalent to take the GDFT with parameter  $\alpha^{-*}$  of  $\tilde{x}_\alpha^*(-n)$ . The proof is given in Appendix E.

Before we proceed with the next property let us define the weighted circular correlation of two in general complex length  $N$  signals,  $x(n)$  and  $y(n)$  by the linear (deterministic) correlation function of  $x(n)$  and  $\tilde{y}_{\alpha^{-*}}(n)$ , i.e.,

$$\begin{aligned} \tilde{r}_{\alpha,xy}(n) &= x(n)*\tilde{y}_{\alpha^{-*}}^*(-n) \\ &= \sum_{m=0}^{N-1} x(m)\tilde{y}_{\alpha^{-*}}^*(m-n) \\ &= \sum_{m=0}^{N-1} x(m)(\alpha^{-p}y^*(m-n+pN)) \\ &= \sum_{m=0}^{N-1} x(m)(\alpha^{-p}y^*((m-n))_N), \end{aligned} \quad (9)$$

where we have used the fact that linear correlation can be expressed in terms of the linear convolution of the signals with one of them time-reversed and conjugated. Note that for  $n = \{0, \dots, N-1\}$  we have,

$$\tilde{r}_{x,xy}(n) = \begin{cases} \sum_{m=0}^{N-1} x(m)y^*(m), & n = 0 \\ \alpha^{-1} \sum_{m=0}^{n-1} x(m)y^*(N+m-n) \\ + \sum_{m=n}^{N-1} x(m)y^*(m-n), & \text{otherwise.} \end{cases} \quad (10)$$

Let us now state the following property.

**Property 7.** *Weighted circular correlation.*

$$\tilde{r}_{x,xy}(n) \xleftrightarrow{\mathcal{F}_z} R_{x,xy}(k) = X_\alpha(k)Y_{\alpha^{-*}}^*(k),$$

where by definition  $R_{x,xy}(k)$  is the GDFD of  $\tilde{r}_{x,xy}(n) = x(n) * \tilde{y}_{\alpha^{-*}}^*(-n)$ . The proof of this property follows directly from the complex-conjugate property (Property 6) with  $\alpha \rightarrow \alpha^{-*}$ , the weighted circular convolution property (Property 1), and Eq. (9).

In analogy to the weighted circular convolution property a weighted circular correlation can be obtained by point-wise multiplication of the spectra in the GFD. However in this case one of the two spectra corresponds to the complex conjugate of the GDFD of the signal with parameter  $\alpha^{-*}$ . Notice that when  $|\alpha| = 1$  we have,

$$\tilde{r}_{x,xy}(n) \xleftrightarrow{\mathcal{F}_z} R_{x,xy}(k) = X_\alpha(k)Y_\alpha^*(k),$$

this includes the standard DFT correlation theorem ( $\alpha = 1$ ).

The following property is a direct consequence of the weighted circular correlation theorem.

**Property 8.** *Parseval's energy relation.*

$$\sum_{n=0}^{N-1} x(n)y^*(n) = \frac{1}{N} \sum_{k=0}^{N-1} X_\alpha(k)Y_{\alpha^{-*}}^*(k). \quad (11)$$

This equality represents Parseval's theorem for the GDFD. It follows by evaluating  $\mathcal{F}_z^{-1}\{R_{x,xy}\} = \tilde{r}_{x,xy}(n)$  at  $n=0$ . For the case  $y(n) = x(n)$  we further have,

$$\sum_{n=0}^{N-1} |x(n)|^2 = \frac{1}{N} \sum_{k=0}^{N-1} X_\alpha(k)X_{\alpha^{-*}}^*(k). \quad (12)$$

The energy in the finite duration signal  $x(n)$  is expressed in terms of the frequency components  $\{X_\alpha(k)X_{\alpha^{-*}}^*(k)\}_{k=0}^{N-1}$ . From here we see that if  $|\alpha| = 1$  the energy in  $x(n)$  equals  $1/N$  times the energy in  $X_\alpha(k)$  i.e.,

$$\sum_{n=0}^{N-1} |x(n)|^2 = \frac{1}{N} \sum_{k=0}^{N-1} |X_\alpha(k)|^2 \quad \text{for all } \alpha : |\alpha| = 1. \quad (13)$$

#### 4. A spatial-audio signal processing application.

In this section we consider the simulation of room impulse responses as an application for the GFD-framework just presented. Let us start with the sound field inside a box-shaped room which always contains reverberation (at least in the vast majority of real-life cases). If the source of sound is perfectly omnidirectional

(a monopole) and produces a perfect delta pulse at a certain time, then the resulting sound field measured at a single point in space is called the room impulse response (RIR) [4,5]. Current approaches to model the sound field in a room although accurate are computationally complex [4,6–9]. In the context of spatial-audio applications like virtual reality systems, real-time or interactive simulation of RIRs at all positions in a room becomes a challenging problem.

Consider now a room with fully reflective walls. In this case, the sound field inside the room is given by a *periodic summation* of the sound field of the source [10]. Intuitively this summation represents the effect of reverberation, since the reflections of the sound field produced by the source(s) on the walls can be modeled by spatial copies of the sources outside the room. If a room could have fully reflective walls, these copies would be perfect and the summation would be perfectly periodic. A key observation to derive a fast algorithm to model the sound field in a room is then the following, *sampling of a function results in a periodic summation of its Fourier transform*. This relation is given by the Poisson summation formula [2,1] and it is a well known property in digital signal processing (see, e.g. [3]). If we carefully sample the spatio-temporal spectrum of the sound field produced by the source and apply an inverse Fourier transform on this sampled spectrum we can obtain the required periodic summation that constitutes the sound field in the whole room [10]. Using this method we dramatically reduce the complexity needed to compute individual impulse responses from  $\mathcal{O}(N_t^3)$  per receiver position (with  $N_t$  proportional to the desired reverberation time  $T_{60}$ ) of approaches related or based on the mirror image source method [7], to  $\mathcal{O}(N_\omega \log(N_\omega))$  (with  $N_\omega$  proportional to the maximum desired temporal bandwidth say,  $\omega_b$ ) taking advantage of the FFT. On the other hand in virtually all real-life cases the walls in a room are at least partially absorptive, the summation defining the sound field in a room is therefore never perfectly periodic. Using standard Fourier theory is however impossible to obtain something different than a periodicity-sampling relation in reciprocal domains. And therefore although of theoretical importance, the method in [10] has no direct practical use.

If the walls are no longer fully reflective in [11] is shown that the sound field in the room can be modeled by a *weighted periodic summation*, of the form given by the generalized Poisson summation formula [1] (in this paper a discrete version of the formula is given by (3)). Every time the sound field is reflected on a wall, part of its energy is absorbed and its frequency components might experience a phase change. Higher order reflections can then be seen as geometrically weighted copies of the sound field of the source. A GFD based method for the simulation of RIRs is then derived as follows. For every source in the room first and second-order reflections on orthogonal walls [10,11] are considered first. To model these, another seven virtual sources are added at positions outside the room. A total of eight *mother sources* are then considered. The sound field of each mother source is then factored into waves traveling only in the direction of each of the eight space octants. This gives rise to a total of  $2^{(3 \times 2)}$

spatio-temporal functions to be considered. Let  $p_{lq}(\mathbf{x}, t)$  represent these functions where  $l = \{0, \dots, 7\}$  is the mother source index and  $q = \{0, \dots, 7\}$  is an enumeration of the octants,  $\mathbf{x} = [x, y, z]^T$  is the space variable vector where the superscript  $T$  denotes matrix transposition, and  $t \in \mathbb{R}$  denotes time. The reverberated sound field in the room is then modeled by [11],

$$p(\mathbf{x}, t) = \sum_{l=0}^7 \sum_{q=0}^7 Q_{lq} \sum_{\mathbf{n} \in \mathbb{Z}^3} \left( \prod_{i \in \{x, y, z\}} Q_i^{\pm n_i} \right) p_{lq}(\mathbf{x} + \mathbf{\Lambda n}, t), \quad (14)$$

where  $\mathbf{\Lambda}$  is the generator matrix of the periodicity lattice  $\Lambda$  (i.e. the multidimensional signal “period”),  $Q_{lq}$  are constants required,  $\mathbf{n} = [n_x, n_y, n_z]$  is a triplet of integers,  $Q_i$ , for  $i \in \{x, y, z\}$  are the reflection factors of the walls, e.g.  $\rho_x = \rho_{x0} \rho_{x1}$  where  $Q_{x0}$  is the reflection factor of the wall perpendicular to the  $x$  direction at the origin of coordinates and  $Q_{x1}$  the reflection factor of the opposite wall. The sign of the exponent in the product over  $i \in \{x, y, z\}$  depends on the particular octant in the definition of the function  $Q_{lq}$ . The reader is referred to [11] for the details of this derivation. The important result behind (14) is that the infinite summation over  $\mathbf{n}$  is a *weighted periodic summation*, of the form given by the generalized Poisson summation formula, which for multidimensional signals takes the form,

$$\sum_{\mathbf{n} \in \mathbb{Z}^v} \left( \prod_{i=0}^{v-1} \alpha_i^{n_i} \right) p(\mathbf{x} + \mathbf{\Lambda n}) = \frac{e^{-\boldsymbol{\beta}^T \mathbf{x}}}{|\mathbf{\Lambda}|} \sum_{\mathbf{k} \in \mathbb{Z}^v} P_{\boldsymbol{\alpha}}(\mathbf{\Phi k}) e^{j(\mathbf{k}^T \mathbf{\Phi}^T \mathbf{x})}, \quad (15)$$

where  $v \in \mathbb{Z}$  is the dimension of the space,  $|\mathbf{\Lambda}|$  is the absolute value of the determinant of  $\mathbf{\Lambda}$ ,  $\mathbf{\Phi} = 2\pi\mathbf{\Lambda}^{-T}$  is the generator matrix of the spectral sampling lattice  $\Phi$  (the (scaled) reciprocal lattice of the periodicity lattice  $\Lambda$ ),  $\boldsymbol{\beta} = \mathbf{\Lambda}^{-T} \mathbf{log}(\boldsymbol{\alpha})$ ,  $\boldsymbol{\alpha} \in \mathbb{C}^v : \alpha_i \neq 0 \forall i = 0, \dots, v-1$ , is the parameter of the multidimensional generalized Fourier transform  $P_{\boldsymbol{\alpha}}$ , and  $\mathbf{log}(\boldsymbol{\alpha}) \triangleq [\log(\alpha_0), \dots, \log(\alpha_{v-1})]^T$ .

The main result in [11] relates the sound field in a room with a sampling condition on the generalized Fourier spectrum. This is, if  $\mathbf{\Lambda}$  denotes the generator matrix of the lattice specifying the spatial periodic packing of the sound fields  $p_{lq}(\mathbf{x}, t)$ , and  $\mathbf{\Phi}$  denotes the generator matrix of the lattice specifying the sampling points of the spatial-generalized spectra, then making  $\mathbf{\Phi} = 2\pi\mathbf{\Lambda}^{-T}$ , the functions  $P_{\boldsymbol{\alpha}lq}(\mathbf{\Phi k}, \omega)$ ,  $\mathbf{k} \in \mathbb{Z}^3$  are the generalized Fourier coefficients of

$$\sum_{\mathbf{n} \in \mathbb{Z}^3} \left( \prod_{i \in \{x, y, z\}} Q_i^{\zeta_q(i)n_i} \right) p_{lq}(\mathbf{x} + \mathbf{\Lambda n}, t), \quad (16)$$

with  $\boldsymbol{\alpha} = [Q_x^{\zeta_q(x)}, Q_y^{\zeta_q(y)}, Q_z^{\zeta_q(z)}, 1]^T$ , where  $\omega$  is the temporal frequency variable and  $\zeta_q(\cdot) = \pm 1$ , depending on the coordinates defining the  $q$ th octant of the space.

To apply the method on a computer, all frequency variables (not only the spatial-frequency variable) must be sampled. Sampling the temporal-frequency variable  $\omega$  introduces temporal aliasing. Let  $\boldsymbol{\Psi}$  be the matrix of the spectral sampling lattice  $\boldsymbol{\Psi} = \text{diag}(\mathbf{\Phi}, \Omega_s)$ ,  $\Omega_s$  is the temporal-frequency sampling interval. Define  $\mathbf{\Delta} = \text{diag}(\mathbf{\Lambda}, T_s)$ , so that  $\boldsymbol{\Psi} = 2\pi\mathbf{\Delta}^{-T} = 2\pi\text{diag}(\mathbf{\Lambda}, T_s)^{-T}$ , where

$T_s = 2\pi / \Omega_s$  is the interval of temporal periodicity. Then

$$\tilde{p}_{\boldsymbol{\alpha}lq}(\mathbf{x}, t) \triangleq \sum_{\mathbf{n} \in \mathbb{Z}^3} \sum_{n \in \mathbb{Z}} \left( \prod_{i \in \{x, y, z\}} Q_i^{\zeta_q(i)n_i} \right) p_{lq}(\mathbf{x} + \mathbf{\Lambda n}, t + T_s n). \quad (17)$$

The summation over  $n \in \mathbb{Z}$ ,  $n \neq 0$ , is the temporal aliasing. We can neglect it making  $\Omega_s \leq 1$ , ( $T_s$  becomes large), this increases computational complexity since a smaller sampling interval implies more samples needed in the reconstruction. Taking advantage of the GFD framework, temporal aliasing can be further reduced using a temporal component different than 1 in the  $\boldsymbol{\alpha}$  parameter of (16), without the need to change the sampling rate. We derive this below, after the current discussion.

The sound field is therefore approximated,

$$p(\mathbf{x}, t) \approx \sum_{l=0}^7 \sum_{q=0}^7 \frac{e^{-\boldsymbol{\beta}_q^T \mathbf{x} - \beta t}}{|\mathbf{\Lambda}|} \sum_{\mathbf{k} \in \mathbb{Z}^4} Q_{lq} P_{\boldsymbol{\alpha}lq}(\boldsymbol{\Psi k}) e^{j(\mathbf{k}^T \boldsymbol{\Psi}^T [\mathbf{x}^T, t]^T)}. \quad (18)$$

Further, the infinite summation over  $\mathbf{k}$  in (18), must be limited to a finite number of elements. Extending periodically this finite set of spectral coefficients, we impose a discretization of the space-time function, so that a sampled (in both space and time) sound field is approximated (which can then be handled on a computer). The spectral set must be big enough to cover the support of the spectrum if corruption due to aliasing is to be avoided.

Let  $\Sigma \subseteq \mathcal{P}$ , be the spectral periodicity lattice, and  $\Gamma$  the spatio-temporal sampling lattice, assume  $\Delta \subseteq \Gamma$ . Then  $\Gamma = 2\pi\Sigma^{-T}$ , so that,

$$\tilde{p}_{\boldsymbol{\alpha}lq}(\Gamma \mathbf{n}) = \frac{e^{-\boldsymbol{\beta}^T \Gamma \mathbf{n}}}{N(\Delta/\Gamma)} \sum_{\mathbf{k} \in V_{\Sigma}(\mathbf{0})} |\Gamma|^{-1} P_{\boldsymbol{\alpha}lq}(\boldsymbol{\Psi k}) e^{j(\mathbf{k}^T \boldsymbol{\Psi}^T \Gamma \mathbf{n})}, \quad (19)$$

where  $V_{\Sigma}(\mathbf{0})$  is the (central) Voronoi region around the origin of lattice  $\Sigma$ ,  $N(\Delta/\Gamma)$  is the number of lattice points of  $\Gamma$  that lie in  $V_{\Delta}(\mathbf{0})$  (the central Voronoi region of lattice  $\Delta$ ). Making  $V_{\Sigma}(\mathbf{0})$  larger implies a finer sampling of  $\tilde{p}_{\boldsymbol{\alpha}lq}$ . Further we have that,

$$N(\Delta/\Gamma) = \frac{|\mathbf{\Lambda}|}{|\mathbf{\Gamma}|} = \frac{(2\pi)^4 |\boldsymbol{\Psi}^{-T}|}{(2\pi)^4 |\Sigma^{-T}|} = \frac{|\Sigma|}{|\boldsymbol{\Psi}|} = N(\Sigma/\mathcal{P}).$$

The sampled sound field is thus obtained by,

$$p(\Gamma \mathbf{n}) \approx \sum_{l=0}^7 \sum_{q=0}^7 Q_{lq} \tilde{p}_{\boldsymbol{\alpha}lq}(\Gamma \mathbf{n}) \quad \text{for } \Gamma \mathbf{n} \in V_{\Delta}(\mathbf{0}). \quad (20)$$

Considering that the spectrum energy is concentrated in  $\|\boldsymbol{\phi}\| \leq |\omega/c|$  [12] we can evaluate up to a given  $\omega_b$ . Note that (19) has the form of a generalized Poisson summation formula (the multidimensional extension of (3)), the right hand term is thus a multidimensional GDFT and the inner summation over  $\mathbf{k}$  corresponds to a DFT (this comes from the fact that the GDFT is equivalent to the DFT of the modulated input signal). Using the FFT, the operation will take only  $\mathcal{O}(N_{\omega}^4 \log N_{\omega})$  operations for computing  $N(\Delta/\Gamma)$  spatio-temporal positions, with  $N_{\omega}$  proportional to  $\omega_b$ . Since  $N(\Delta/\Gamma) = N(\Sigma/\mathcal{P})$ , the method is of complexity  $\mathcal{O}(N_{\omega} \log N_{\omega})$  per receiver position. Again the reader is referred to [11] for detailed experimental results.

Returning to Eq. (17), we see that temporal aliasing is introduced due to spectral sampling of  $\omega$ . Clearly, by making the spectral sampling period  $\Omega_s$  smaller, the

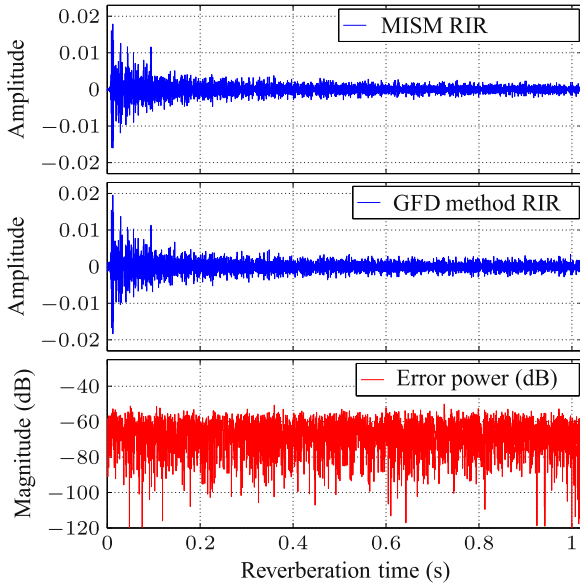


Fig. 2. Simulated room impulse responses.

aliasing components in the time dimension appear further apart from each other, reducing the error. In time the RIR does not have compact support, but it is a *causal* (single sided) function, having a starting point in time and an exponential decay afterwards (see e.g. [5] for a parametric characterization of this decay). A simulated example RIR using the Mirror Image Source Method (MISM) [7], is depicted in Fig. 2, together with a RIR simulated using the GFD approach described above and in [11], the error power between both signals is plotted in dB. The bandwidth frequency is  $\omega_b = 2\pi(2 \text{ kHz})$ , so that the temporal sampling frequency is  $f_s = 4 \text{ kHz}$ . The length of the RIR is  $T_h = 1.02 \text{ s}$  or 4096 taps. The GFD method RIR shown in Fig. 2 is obtained according to (19) and (20) using a parameter  $\alpha = [Q_x^{c_q(x)}, Q_y^{c_q(y)}, Q_z^{c_q(z)}, 1]^T$ , so that the spatial part of the  $\alpha$  parameter applied in the generalized Fourier synthesis gives the required spatial weighted periodicity, and in time a standard Fourier synthesis is applied. The RIR is thus one spatial sample of the set  $p(\Gamma\mathbf{n})$ . The spectral sampling period is set to  $\Omega_s = 2\pi/(2T_h)$ , so that the interval of temporal periodicity (and thus temporal aliasing)  $T_s$  is 2 times the reverberation time.

Using a temporal component  $\alpha_t \neq 1$  in the  $\alpha$  parameter, we can further reduce the temporal aliasing. Since the RIR is a causal function of time, the repeated terms to the right of the temporal support of the RIR (for  $n < 0$ ), do not contribute to the time-domain aliasing. Therefore we can rewrite (17) as,

$$\begin{aligned} \tilde{p}_{\alpha lq}(\mathbf{x}, t) &= \sum_{\mathbf{n} \in \mathbb{Z}^3} \left( \prod_{i \in \{x,y,z\}} Q_i^{c_q(i)n_i} \right) p_{lq}(\mathbf{x} + \mathbf{A}\mathbf{n}, t) \\ &+ \sum_{n=1}^{\infty} \sum_{\mathbf{n} \in \mathbb{Z}^3} (\alpha_t^n) \left( \prod_{i \in \{x,y,z\}} Q_i^{c_q(i)n_i} \right) p_{lq}(\mathbf{x} + \mathbf{A}\mathbf{n}, t + T_s n). \end{aligned} \quad (21)$$

In principle by making e.g.  $\alpha_t \ll 1$  we can further reduce the temporal aliasing without the need to increase the spectral sampling period  $\Omega_s$ . In practice however, the accuracy of the computations is limited by the arithmetic precision used, moreover the causality of the RIR in time is only strictly valid in non-bandlimited scenarios. This is, by limiting the summation over  $\mathbf{k}$  in (18) to a finite number of elements, we are effectively multiplying the discrete spatio-temporal spectrum by a multidimensional rectangular window. In space-time this has the effect of a convolution with a multidimensional sinc function, making the resulting band-limited RIR non-causal. In this case (17) for  $n \neq 0$  defines the aliasing terms, but still the terms for  $n < 0$  have less corruptive influence. Despite these practical issues it is still possible to reduce the temporal aliasing using a temporal component e.g.  $\alpha_t \ll 1$  in the generalized Fourier synthesis (19). In Fig. 3(a)–(d) results of the generalized Fourier synthesis are given setting  $\alpha_t = 0.5$ ,  $\alpha_t = 10^{-2}$ ,  $\alpha_t = 10^{-3}$  and  $\alpha_t = 10^{-4}$  respectively. Indeed aliasing corruption decreases for the first two cases, but for  $\alpha_t = 10^{-3}$  and  $\alpha_t = 10^{-4}$  the repeated terms to the right of the temporal support of the RIR become too large, having a negative impact in the reconstruction. Clearly the corruption is more pronounced to the right of the support of the RIR. In this case setting the parameter  $\alpha_t = 10^{-2}$  gives a good reconstruction, especially when compared with the result obtained setting  $\alpha_t = 1$  depicted in Fig. 2. Working in the GFD on the temporal dimension allows a non-negligible gain in accuracy.

The method for multichannel simulation of RIRs has an important application in immersive virtual gaming (using for example stereo headphones). In this case many RIRs for different (virtual) room conditions need to be computed and later fast convolved with a given audio signal (i.e. auralization) to give the users an audio experience such that they have the impression of being in the game field. For example, at one moment the users could be at an open location such as a park, and at another moment they could be inside a room. To create a satisfactory experience, the system have to reproduce the acoustic characteristics of different scenarios for moving sources/receivers. The computation of all the necessary RIRs can be done with low-complexity using the GFD method presented in [11]. A GDFT in the temporal dimension can be applied to reduce aliasing corruption as explained above. The novel GFD framework presented in this paper can then be used to perform fast convolution for auralization or other signal processing tasks in the GFD.

## 5. Concluding remarks

In this work, a generalized Fourier domain (GFD) signal processing framework is introduced. The proposed framework allows a special form of control on the periodic repetitions that occur due to sampling in the reciprocal domain. We show that this property can be expressed in terms of a *weighted periodic extension* of a signal. We demonstrate that the (discrete-time) generalized Fourier transform can be seen as a special case of the z-transform, and relate the analytic continuation of the standard Fourier spectrum to the generalized Fourier spectrum.

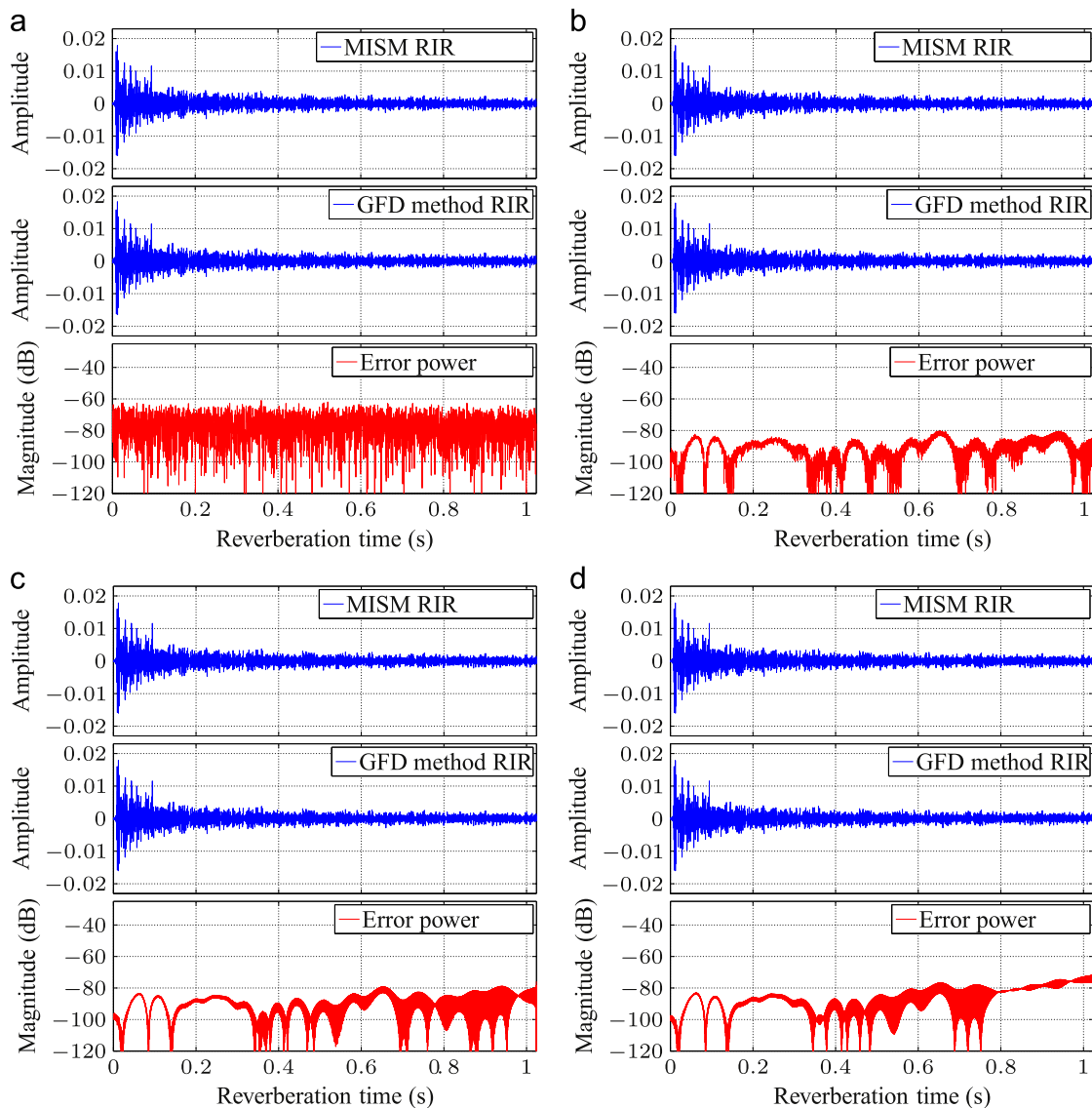


**Fig. 3.** Comparison of RIRs simulated with the GFD method setting parameter  $\alpha_t$  to different values, and the same RIR simulated with the MISM depicted in Fig. 2. (a)  $\alpha_t = 0.5$ , (b)  $\alpha_t = 10^{-2}$ , (c)  $\alpha_t = 10^{-3}$ , (d)  $\alpha_t = 10^{-4}$ .

Core properties of the generalized discrete Fourier transform (GDFT) are given. These allow to concisely work in the GFD. The close relationship of the GDFT to the DFT allows a generalized fast Fourier transform (GFFT) to be directly obtained via the FFT.

The novel framework opens possibilities for signal processing applications where working on the GFD results in a computational or analytical advantage. As an example, we review a method for low-complexity simulation of room impulse responses (RIRs) [10,11] based on the GFD. The framework presented in this paper can then be used to perform e.g. auralization, adaptive filtering or other acoustic signal processing operations in the GFD.

MATLAB<sup>®</sup> code to implement the GDFT is available online for educational and non-profit purposes at the webpage of TuDelft SIPLAB (<http://siplab.tudelft.nl>).

## Appendix A. Proof of Property 2

**Proof.** Time-domain shift property.

For  $n_0 \in \mathbb{Z}$ , we have that

$$\tilde{x}_\alpha(n-n_0) = \alpha^p x((n-n_0)_N) = \alpha^p x(n-n_0+pN),$$

where  $p = -\lfloor (n-n_0)/N \rfloor$ . Then,

$$\begin{aligned} \mathcal{F}_\alpha\{\tilde{x}_\alpha(n-n_0)\} &= \sum_{n=0}^{N-1} \tilde{x}_\alpha(n-n_0) e^{\beta n} e^{-j(2\pi/N)kn} \\ &= \sum_{n=0}^{N-1} \alpha^p x(n-n_0+pN) e^{\beta n} e^{-j(2\pi/N)kn}, \end{aligned}$$

make  $m = n - n_0 + pN$ , then

$$\begin{aligned} \mathcal{F}_\alpha\{\tilde{x}_\alpha(n - n_0)\} &= \sum_{m=0}^{N-1} \alpha^p x(m) e^{\beta(m+n_0-pN)} e^{-j(2\pi/N)k(m+n_0-pN)} \\ &= e^{\beta n_0} e^{-j(2\pi/N)kn_0} \sum_{m=0}^{N-1} x(m) e^{\beta m} e^{-j(2\pi/N)km} \\ &= e^{\beta n_0} e^{-j(2\pi/N)kn_0} X_\alpha(k). \quad \square \end{aligned}$$

$$\begin{aligned} &= \left( \sum_{n=0}^{N-1} x(n) e^{\beta n} e^{j(2\pi/N)kn} \right)^* \\ &= \left( \sum_{n=0}^{N-1} x(n) e^{\beta n} e^{-j(2\pi/N)(N-k)n} \right)^* \\ &= \tilde{X}_\alpha^*(-k). \quad \square \end{aligned}$$

## Appendix B. Proof of Property 3

**Proof.** GFD shift property.

For  $k_0 \in \mathbb{Z}$ ,

$$\begin{aligned} \mathcal{F}_\alpha\{x(n) e^{j(2\pi/N)k_0 n}\} &= \sum_{n=0}^{N-1} x(n) e^{j(2\pi/N)k_0 n} e^{\beta n} e^{-j(2\pi/N)kn} \\ &= \sum_{n=0}^{N-1} x(n) e^{\beta n} e^{-j(2\pi/N)n(k-k_0)} \\ &= \sum_{n=0}^{N-1} x(n) e^{\beta n} e^{-j(2\pi/N)n(k-k_0)_N} \\ &= X_\alpha((k-k_0)_N) = \tilde{X}_\alpha(k-k_0). \quad \square \end{aligned}$$

## Appendix C. Proof of Property 4

**Proof.** Time reversal.

For

$$\tilde{x}_\alpha(-n) = \begin{cases} x(n) & \text{for } n = 0 \\ \alpha x(N-n) & \text{for } n = \{1, \dots, N-1\}, \end{cases}$$

we have that,

$$\mathcal{F}_{\alpha^{-1}}\{\tilde{x}_\alpha(-n)\} = x(0) + \sum_{n=1}^{N-1} \alpha x(N-n) e^{-\beta n} e^{-j(2\pi/N)kn},$$

set  $m = N-n$ , then,

$$\begin{aligned} \mathcal{F}_{\alpha^{-1}}\{\tilde{x}_\alpha(-n)\} &= x(0) + \sum_{m=1}^{N-1} \alpha x(m) e^{-\beta(N-m)} e^{-j(2\pi/N)k(N-m)} \\ &= x(0) + \sum_{m=1}^{N-1} x(m) e^{\beta m} e^{-j(2\pi/N)(N-k)m} \\ &= \sum_{m=0}^{N-1} x(m) e^{\beta m} e^{-j(2\pi/N)(N-k)m} \\ &= X_\alpha(N-k) = \tilde{X}_\alpha(-k), \end{aligned}$$

since  $\beta = \log(\alpha)/N$ .  $\square$

## Appendix D. Proof of Property 5

**Proof.** Time domain complex-conjugate.

$$\mathcal{F}_{\alpha^*}\{x^*(n)\} = \sum_{n=0}^{N-1} x^*(n) e^{\beta^* n} e^{-j(2\pi/N)kn}$$

## Appendix E. Proof of Property 6

**Proof.** GFD complex-conjugate.

$$\begin{aligned} \mathcal{F}_{(\alpha^*)^{-1}}\{X_\alpha^*(k)\} &= \frac{e^{\beta^* n}}{N} \sum_{k=0}^{N-1} X_\alpha^*(k) e^{j(2\pi/N)kn} \\ &= \frac{e^{\beta^* n}}{N} \left( \sum_{k=0}^{N-1} X_\alpha(k) e^{-j(2\pi/N)kn} \right)^* \\ &= \begin{cases} x^*(0), & n = 0 \\ e^{\beta^* n} x^*(N-n) e^{\beta^*(N-n)}, & \text{otherwise} \end{cases} \\ &= \begin{cases} x^*(0), & n = 0 \\ (\alpha x(N-n))^*, & \text{otherwise} \end{cases} \\ &= \tilde{x}_\alpha^*(-n), \end{aligned}$$

since  $\beta = \log(\alpha)/N$ .  $\square$

## References

- [1] J. Martinez, R. Heusdens, R.C. Hendriks, A generalized Poisson summation formula and its application to fast linear convolution, *IEEE Signal Processing Letters* 18 (9) (2011) 501–504.
- [2] R. Bracewell, *The Fourier Transform & Its Applications*, 3rd edition, McGraw-Hill, New York, 1999.
- [3] J.G. Proakis, D.G. Manolakis, *Digital Signal Processing, Principles, Algorithms and Applications*, 4th edition, Prentice-Hall, New York, 2007.
- [4] H. Kuttruff, *Room Acoustics*, Taylor and Francis, London, U.K., 2000.
- [5] Y. Huang, J. Benesty, J. Chen, *Acoustic MIMO Signal Processing (Signals and Communication Technology)*, Springer-Verlag, Secaucus, NJ, 2006.
- [6] B. Xu, S.D. Sommerfeldt, A hybrid modal analysis for enclosed sound fields, *Journal of the Acoustical Society of America* 128 (5) (2010) 2857–2867.
- [7] J. Allen, D. Berkley, Image method for efficiently simulating small room acoustics, *Journal of the Acoustical Society of America* 65 (1979) 943–950.
- [8] A. Berkhout, D. de Vries, J. Baan, B. van den Oetelaar, A wave field extrapolation approach to acoustical modeling in enclosed spaces, *Journal of the Acoustical Society of America* 105 (1999) 1725–1733.
- [9] S.R. Bistafa, J.W. Morrissey, Numerical solutions of the acoustic eigenvalue equation in the rectangular room with arbitrary (uniform) wall impedances, *Journal of Sound and Vibration* 263 (1) (2003) 205–218.
- [10] J. Martinez, R. Heusdens, On low-complexity simulation of multi-channel room impulse responses, *IEEE Signal Processing Letters* 17 (7) (2010) 667–670.
- [11] J. Martinez, R. Heusdens, R.C. Hendriks, A spatio-temporal generalized fourier domain framework to acoustical modeling in enclosed spaces, in: *Proceedings of the ICASSP*, 2012, pp. 529–532.
- [12] T. Ajdler, L. Sbaiz, M. Vetterli, The plenacoustic function and its sampling, *IEEE Transactions on Signal Processing* 54 (10) (2006) 3790–3804.